nature genetics

Mitochondrial aging is accelerated by anti-retroviral therapy through the clonal expansion of mtDNA mutations

Brendan A I Payne[1,2], Ian J Wilson[1], Charlotte A Hateley[1], Rita Horvath[1], Mauro Santibanez-Koref[1], David C Samuels[3], D Ashley Price[2] & Patrick F Chinnery[1]

There is emerging evidence that people with successfully treated HIV infection age prematurely, leading to progressive multi-organ disease[1], but the reasons for this are not known. Here we show that patients treated with commonly used nucleoside analog anti-retroviral drugs progressively accumulate somatic mitochondrial DNA (mtDNA) mutations, mirroring those seen much later in life caused by normal aging[2,3]. Ultra-deep re-sequencing by synthesis, combined with single-cell analyses, suggests that the increase in somatic mutation is not caused by increased mutagenesis but might instead be caused by accelerated mtDNA turnover. This leads to the clonal expansion of preexisting age-related somatic mtDNA mutations and a biochemical defect that can affect up to 10% of cells. These observations add weight to the role of somatic mtDNA mutations in the aging process and raise the specter of progressive iatrogenic mitochondrial genetic disease emerging over the next decade.

Somatic mtDNA mutations accumulate in individual cells during normal human aging, leading to cellular bio-energetic defects of oxidative phosphorylation[2,4]. Transgenic mice with a defective mtDNA polymerase (pol γ) accumulate secondary mtDNA mutations and a prematurely aged phenotype[3], but it is still not clear whether the mtDNA mutations are a cause or a consequence of aging in humans. Accelerated senescence has recently been described in humans with successfully treated HIV infection[1]. These patients become frail at an early age, decline physiologically[5,6] and acquire age-associated degenerative disorders affecting the cardiovascular system and the brain leading to dementia[7,8]. Several nucleoside analog reverse transcriptase inhibitor anti-retroviral drugs (NRTIs) used in the treatment of HIV inhibit the function of pol γ[9], raising the possibility that drug treatment contributes to the accelerated aging phenotype through mtDNA damage. NRTIs are well known to cause an acute, temporary and reversible reduction in the amount of mtDNA (mtDNA depletion), and one previous study detected mtDNA deletions in patients being actively treated with NRTIs[10–12]. However, no previous studies have looked at the possibility of irreversible long-term effects of the drugs on mtDNA mutations after NRTI treatment has ceased.

We studied skeletal muscle from 33 HIV-infected adults, all aged 50 years or under, stratified by lifetime exposure to NRTIs previously shown to affect pol γ *in vitro*[9] (Online Methods and **Supplementary Table 1**), and 10 HIV-uninfected healthy controls (HIV−) of comparable age. We initially looked for a defect of mitochondrial oxidative phosphorylation within individual cells using cytochrome *c* oxidase–succinate dehydrogenase (COX-SDH) histochemistry. Cellular COX defects would not be expected in this younger subject group (<0.5%)[4].The frequency of COX-deficient muscle fibers in HIV-infected non-treated (treatment-naïve, HIV+/NRTI−) subjects ($n = 12$) was indistinguishable from that observed in HIV− controls, with the majority having no COX-deficient fibers. By contrast, NRTI-exposed (HIV+/NRTI+) subjects ($n = 21$) had an increased frequency of COX-deficient muscle fibers (maximum 9.8%, $P = 0.047$), reaching or exceeding levels expected in healthy elderly individuals[4] (**Fig. 1**). The severity of the COX defect was strongly predicted by cumulative lifetime NRTI exposure, rather than therapy at the time of study, implicating a persistent and cumulative mitochondrial defect ($r^2 = 87\%$, $P < 0.001$; **Supplementary Fig. 1**).

We then defined the molecular basis for the COX deficiency observed in NRTI-exposed subjects. We first excluded persistent mtDNA depletion. The mtDNA content in homogenized skeletal muscle did not differ between HIV+/NRTI+ and HIV+/NRTI− patients (**Supplementary Fig. 2**). In keeping with this, the analysis of individual laser-captured single muscle fibers ($n = 128$) showed that only a small minority of COX-deficient fibers (6 out of 70, or 9%) from NRTI-treated patients had mtDNA depletion compared to adjacent fibers with normal COX activity. By contrast, the vast majority of the isolated COX-deficient fibers contained markedly increased amounts of mtDNA (geometric mean of 2.1-fold proliferation, maximum 21.3-fold; $P < 0.001$ for difference in mean mtDNA content between COX-deficient and normal fibers) (**Fig. 2a**). Focal mtDNA proliferation is often seen in association with pathogenic mtDNA mutations. In keeping with this, the majority of the COX-deficient fibers analyzed (40 out of 70 fibers from 12 HIV+/NRTI+ patients) showed high percentage levels of mtDNA molecules containing large-scale deletion mutations, exceeding the percentage level of mutation

[1]Mitochondrial Research Group, Institute of Genetic Medicine, Newcastle University, Newcastle-upon-Tyne, UK. [2]Department of Infection and Tropical Medicine, Royal Victoria Infirmary, Newcastle-upon-Tyne, UK. [3]Centre for Human Genetics Research, Vanderbilt University, Nashville, Tennessee, USA. Correspondence should be addressed to P.F.C. (p.f.chinnery@ncl.ac.uk).

Received 8 February; accepted 23 May; published online 26 June 2011; doi:10.1038/ng.863

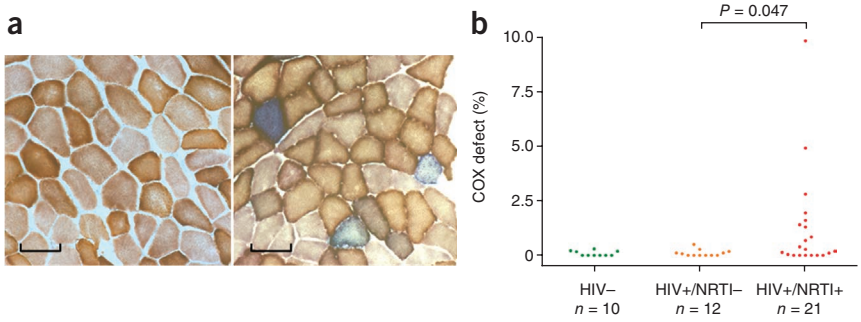

Figure 1 COX (cytochrome *c* oxidase) deficiency in single skeletal muscle fibers. (**a**) COX histochemistry from a representative healthy control subject (HIV–) showing normal COX activity, whereas a nucleoside analog treated HIV-infected patient (HIV+/NRTI+) shows multiple COX-deficient fibers (counterstained blue by residual SDH (succinate dehydrogenase) activity). Scale bars, 100 µm.(**b**) COX defects observed in each subject group (HIV+/NRTI–, HIV-infected treatment-naïve subjects; each dot represents an individual patient biopsy; ≥500 fibers sampled per biopsy).

required to cause a COX defect (~60%[13]). We detected no deletion mutations in adjacent skeletal muscle fibers (n = 58) with normal COX activity. Analysis of the mtDNA deletion break points (n = 15 fibers from four HIV+/NRTI+ patients) revealed different deletions in different fibers, all of which were clonal within individual fibers. Most of the clonally expanded deletions were unique; the only deletion observed more than once was the mt.δ4977 'common deletion', the commonest age-associated somatic mtDNA mutation[14,15] (**Fig. 2b**,**c** and **Supplementary Table 2**).

Although less common than large-scale deletion mutations, mtDNA point mutations are also found in COX-deficient fibers from healthy aged subjects[16]. In keeping with this, in the NRTI-treated patients, we found COX-deficient fibers not containing a deletion to harbor non-synonymous somatic mtDNA point mutations (5 out of 29 fibers). These mutations are predicted to alter a highly conserved amino acid and have not previously been described as inherited polymorphic variants in 5,140 humans (**Table 1**) (one variant, 12797T>C, had been observed as a somatic variant in a single human sequence)[17] and thus provide an explanation for the associated cellular COX defect. Other fibers contained high levels of noncoding control-region (nt 16,024 to nt 576) variants, which were previously described in healthy aged humans.

We then estimated the total burden of mtDNA deletion mutations at the whole-tissue level. The proportion of mtDNA molecules containing the mt.δ4977 'common deletion' was significantly higher in NRTI-treated patients compared with untreated patients (HIV+/NRTI+ (mean ± s.e.m.), -3.45 ± 0.25 $\log_{10}$(/mtDNA); HIV+/NRTI–, -4.56 ± 0.31 $\log_{10}$(/mtDNA); $P = 0.012$) (**Fig. 3**) and were comparable with those previously reported in very elderly healthy subjects[18]. Furthermore, the proportion of COX-deficient muscle fibers from NRTI-treated subjects which contained mt.δ4977 was very similar to that reported in healthy aged individuals[15]. Pathogenic mutations within single fibers (of which the majority were deletions) were accompanied by proliferation of mtDNA, which occurs in an attempt to maintain adequate levels of wild-type mtDNA, as shown previously[19]. As a result, mutated mtDNA also proliferates within the fiber. Over time, this will lead to a detectable increase in the level of deletions at the whole-tissue level.

To estimate the relative burden of mtDNA point mutations between treatment groups in homogenized skeletal muscle, we designed an ultra-deep re-sequencing by synthesis (UDS) assay using FLX GS technology (Roche 454). First, we carried out a series of control experiments to show the sensitivity of UDS to detect mtDNA point variants. We initially established that UDS of an mtDNA template did not generate an intrinsically different signal when compared to a nuclear DNA template by sequencing amplicons of cloned autosomal and mitochondrial DNA fragments as well as an autosomal DNA amplicon from genomic DNA (**Supplementary Table 3**). By this approach, we confirmed a very low background noise level for the UDS assay (Online Methods and **Supplementary Fig. 3**). As a positive control, we then compared two mtDNA amplicons from skeletal muscle DNA of *POLG* patients (n = 4), individuals known to harbor high levels of somatic mtDNA point mutations[20,21]. One mtDNA amplicon was in the hypervariable noncoding control region (*MT-HV2*) predicted from 5,140 population-level sequences[17] to have a high mutation rate,

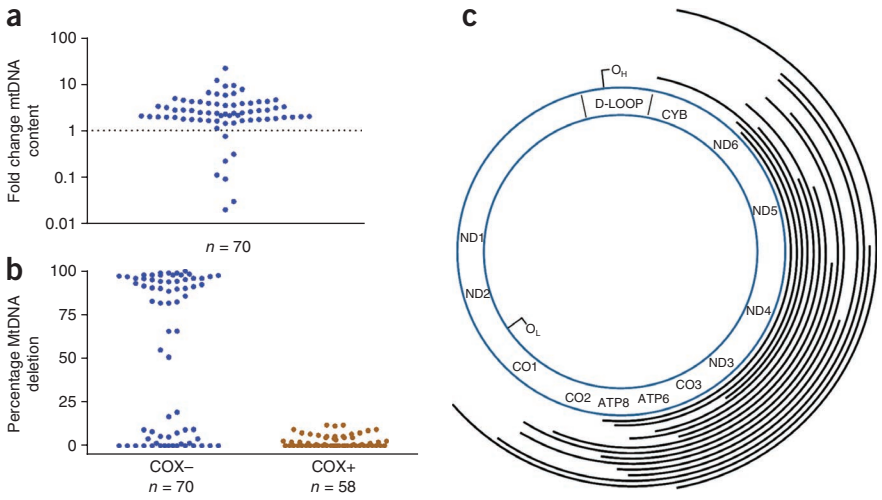

Figure 2 Mitochondrial DNA analysis of single skeletal muscle fibers. (**a**) Mitochondrial DNA (mtDNA) content in individual COX (cytochrome *c* oxidase)-deficient muscle fibers from nucleoside analog treated HIV-infected (HIV+/NRTI+) subjects, expressed relative to mtDNA content in adjacent fibers of normal COX activity from the same subject. A few fibers show reduced mtDNA content, whereas the majority show increased content (geometric mean of 2.1-fold proliferation, maximum 21.3-fold; $P < 0.001$ for difference in mean mtDNA content between COX-deficient and normal fibers). (**b**) The majority of COX-deficient fibers (COX–) contained high percentage levels of mtDNA containing a large-scale deletion of the major arc, causing the COX defect; whereas no deleted mtDNA was detected in adjacent COX positive fibers (COX+) ($P < 0.001$). (**c**) Schematic representation of mtDNA large-scale deletion breakpoints in COX-deficient fibers from HIV+/NRTI+ patients relative to the mtDNA gene positions (transfer RNA and ribosomal RNA not shown). Each line represents an individual deleted region. O_L, origin of light chain replication; O_H, origin of heavy chain replication. (n = 15 fibers from four patients).

Table 1 MtDNA somatic point mutations identified by whole mtDNA genome sequencing

Subject	Somatic mutation and variant		Population frequency (in 5,140 sequences)
Likely pathogenic somatic changes in coding region (mt.577–16,023)			
8	m.7818T>C	p.Leu68Pro (*CO2*)	0
8	m.9253G>A	p.Asp15Asn (*CO3*)	0
8	m.12797T>C	p.Leu154Pro (*ND5*)	1[a]
2	m.6579G>A	p.Gly226Ter (*CO1*)	0
11	m.9907G>A	p.Gly234Asp (*CO3*)	0
15	m.6580G>A	p.Gly226Glu (*CO1*)	0
Non-pathogenic somatic changes in coding region (mt.577–16,023)			
8	m.7906C>T	Syn	1
8	m.11467A>G	Syn	608
Somatic changes in control region (mt.16,024–576)			
8	m.408T>A	Noncoding	10
8	m.463CAC>Del	Noncoding	0
2	m.408T>A	Noncoding	10
17	m.408T>A	Noncoding	10
17	m.414T>G	Noncoding	0

MtDNA somatic point mutations identified by whole mtDNA genome sequencing of individual COX (cytochrome *c* oxidase)-deficient skeletal muscle fibers from nucleoside analog (NRTI)-treated HIV-infected subjects where a large-scale mtDNA deletion was not detected in that fiber ($n = 29$ COX-deficient fibers sequenced from seven subjects; subjects identified as in **Supplementary Table 1**). Likely pathogenicity (that is accounting for the cellular COX defect) was ascribed if mutations resulted in an amino acid change within a coding gene at a position which showed high inter-species conservation and is not polymorphic within human populations. Population frequencies were taken from a previous study[17].
[a]One variant, 12797T>C, had been observed only as a somatic variant in a single human sequence[17]. Syn, synonymous.

and one was in a highly conserved mtDNA coding region (*MT-CO3*). Mean coverage was 5,892 sequence reads per amplicon in each direction. Consistent with an error-prone pol γ, these subjects showed an increase in mtDNA point variants detectable at >0.2% frequency in the *MT-HV2* amplicon (OR = 2.33, $P = 0.002$) (**Fig. 4**) when compared to healthy controls ($n = 4$). We detected no increase in variants in the *MT-CO3* amplicon. These findings were confirmed on replicate samples (**Supplementary Fig. 4**). When we studied skeletal muscle mtDNA from the HIV+/NRTI+ subjects ($n = 8$), the overall burden of point variants within each amplicon was indistinguishable from HIV+/NRTI− subjects ($n = 4$) and healthy HIV− controls ($n = 4$), all of comparable age (OR = 1.08, $P = 0.79$ for comparison of HIV+/NRTI+ and HIV− for *MT-HV2*). Furthermore, there was no correlation between COX defect in HIV+/NRTI+ subjects (range up to 10%) and mutation burden on the UDS assay.

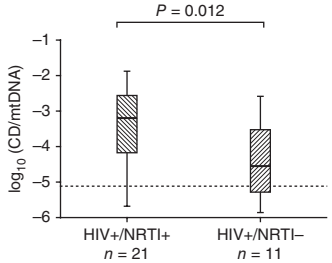

Figure 3 Proportional level of mt.δ4977 'common deletion' (CD) in homogenized skeletal muscle from HIV-infected subjects. HIV+/NRTI+, HIV-infected, nucleoside analog exposed; HIV+/NRTI−, HIV-infected, treatment-naïve. The dashed line represents the lower threshold of the assay. NRTI-treated subjects showed significantly higher mean levels of common deletion than untreated subjects (HIV+/NRTI+ (mean ± s.e.m.), −3.45 ± 0.25 $\log_{10}$(/mtDNA); HIV+/NRTI−, −4.56 ± 0.31 $\log_{10}$(/mtDNA); $P = 0.012$). Box and whisker plot.

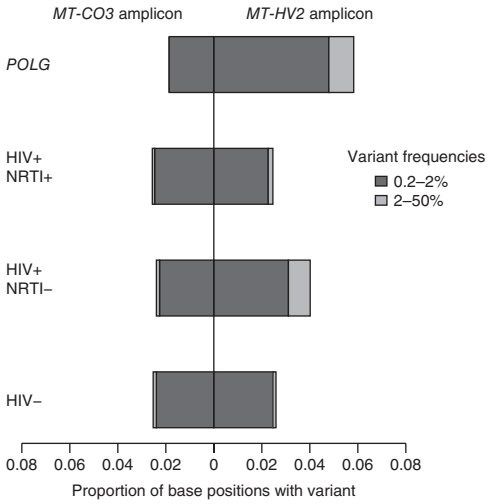

Figure 4 Ultra-deep re-sequencing by synthesis (UDS) of skeletal muscle mtDNA. UDS (Roche 454 FLX GS) shows no difference in burden of low-level mtDNA point variants (exceeding 0.2% frequency) between HIV-infected nucleoside analog treated (HIV+/NRTI+, $n = 8$), HIV-infected treatment-naïve (HIV+/NRTI−, $n = 4$) and control (HIV−, $n = 4$) subjects in two amplicons located in mtDNA hypervariable segment 2 (*MT-HV2*) and mtDNA COX subunit 3 (*MT-CO3*). In contrast, positive control subjects with inherited *POLG* defects (POLG, $n = 4$) show an increased burden of low-level mutations compared with healthy controls in *MT-HV2* (OR = 2.33, $P = 0.002$).

Given that NRTI-treated subjects showed high-level COX defects (up to 10% of fibers) which contained clonal mutated mtDNA species, one explanation for our findings is accelerated segregation of preexisting (age-associated) mtDNA mutations caused by NRTI treatment rather than *de novo* somatic mutation. In contrast, the *POLG* subjects showed a significant increase in point mutation burden in the UDS assay (although only in *MT-HV2*, $P = 0.002$) but a low proportion of COX-deficient fibers. Although the UDS data does not exclude the possibility of a slight increase in mutagenesis in NRTI-exposed subjects, it would not be of the level predicted to be required (>100-fold increase[22]) to cause the observed COX defects.

To determine whether accelerated clonal expansion was a plausible explanation for our findings, we used an established computational model based solely on experimentally derived parameters[22] and simulated the effects of NRTI-induced chain-termination during mtDNA replication[9]. The *de novo* mutation rate was not altered from the original model of aging muscle. A finite NRTI exposure predicted a period of temporary mtDNA depletion which was concordant with reported mtDNA levels[12,23] and the COX defects observed[12] in acutely treated HIV patients. This resulted in accelerated clonal expansion of preexisting mtDNA mutations and led to an irreversible increase in the frequency of COX-deficient muscle fibers (**Fig. 5a**,**b**). The severity of predicted COX defect was dependent on the degree of replication failure and the duration of exposure (**Fig. 5b**,**c**), which is in keeping with our observations in patient muscle that had suggested a strong dependence on these factors (**Supplementary Fig. 1**). *In silico* modeling is thus consistent with the hypothesis that accelerated clonal expansion of preexisting (age-associated) mtDNA somatic mutations is sufficient to explain our observations in NRTI-treated subjects. Having established the model, we explored the effect of timing of NRTI exposure and showed that later periods of therapy predicted a higher frequency of COX deficiency (**Fig. 5d**). This is because of older subjects harboring a greater number of age-related somatic mtDNA mutations than younger subjects, which rapidly clonally segregate

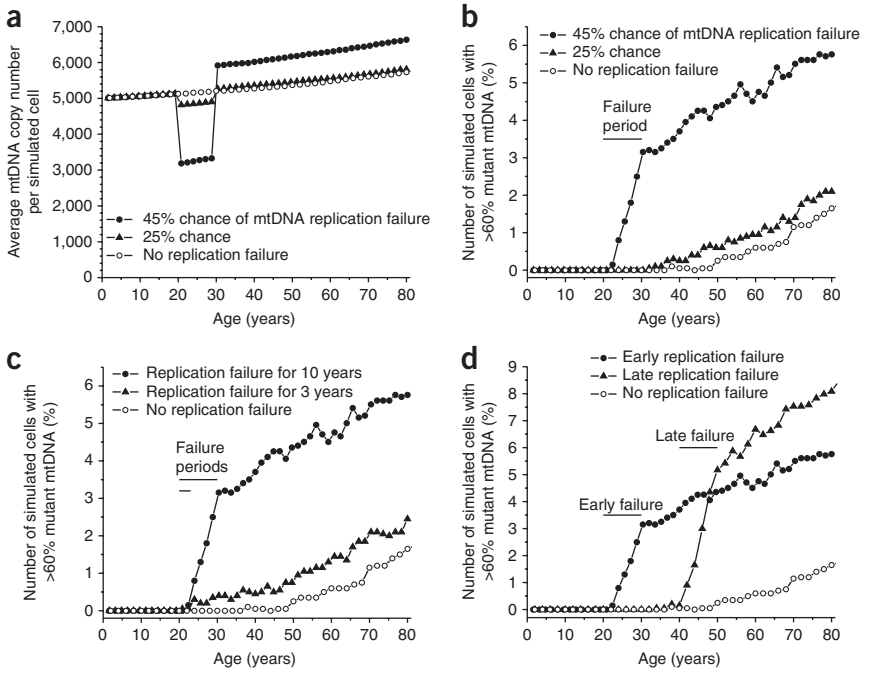

Figure 5 Simulations of the effects of partial mitochondrial DNA (mtDNA) replication failure caused by nucleoside analog (NRTI) exposure. Using a validated computer model of mtDNA replication based solely on experimentally derived parameters[22], we incorporated a finite period of partial replication failure caused by the mtDNA chain-terminating effects of NRTI exposure[9], assigning a probability of failure per mtDNA replication event. All other parameters remained constant, including the *de novo* mutation rate[22]. We simulated 2,000 cells for 80 years. (**a**) The amount of mtDNA depletion during the NRTI exposure period caused by 25% and 45% probability of replication failure between 20 and 30 years of age. (>50% failure led to the complete loss of mtDNA.) The range of mtDNA depletion predicted is in keeping with published *in vivo* data[12,23]. (**b**) This led to a persistent increase in the frequency of COX (cytochrome *c* oxidase)-deficient cells through the accelerated clonal expansion of preexisting somatic mtDNA mutations. (**c**) Direct simulation of the effects of NRTI exposure within our study population (two different periods, 10 and 3 years, starting at age 20, of replication failure with 45% probability). The range of COX defects predicted closely fits our empiric data. (**d**) Late exposure (40–50 years) had a more pronounced effect than early exposure (20–30 years) (with 45% probability of replication failure) caused by the higher number of preexisting (age-related) somatic mtDNA mutations at the time of exposure.

during NRTI therapy. This is in keeping with the observation that mitochondrially mediated clinical complications of NRTI therapy appear to be more common in older individuals[24]. Finally we modeled the longer-term effects of treatment. Using this approach, an HIV-infected individual treated with NRTIs during their third decade is predicted to develop ~5% COX-deficient cells by age 60 (**Fig. 5b–d**). This is similar to or exceeds that seen in the healthy very old[4].

Although the UDS data for mtDNA point mutations support the hypothesis of accelerated clonal expansion of preexisting age-related mutations rather than increased mutagenesis, it is possible that additional mechanisms may be involved for mtDNA large-scale deletions, including a replicative advantage favoring deleted molecules[25]. Furthermore, although UDS provides great depth of mutational analysis, it is analogous to the PCR-cloning method of mutation rate determination and as such will tend to exaggerate an estimate of the mutation rate[26,27].

The rapid clonal expansion of somatic mtDNA mutations we observed in NRTI-treated HIV-infected patients provides a plausible mechanism for accelerated aging in treated HIV infection. This is potentially of great importance for the millions of HIV-infected patients in the developing world where these drugs remain the mainstay of therapy[28] and adds weight to a causal role for somatic mtDNA mutations in human aging.

METHODS

Methods and any associated references are available in the online version of the paper at http://www.nature.com/naturegenetics/.

Note: Supplementary information is available on the Nature Genetics website.

ACKNOWLEDGMENTS

This work was support by grants from the Medical Research Council (B.A.I.P.), British Infection Society (B.A.I.P.), the Newcastle Healthcare Charity (D.A.P.), the UK National Institute for Health Research (NIHR) Biomedical Research Centre for Aging and Age-related disease award to the Newcastle upon Tyne Foundation Hospitals National Health Service (NHS) Trust (P.F.C.) and the Wellcome Trust (P.F.C.). The authors thank G.L. Toms for the use of his containment level 3 facility, E.L.C. Ong, M.L. Schmid, U. Schwab and R. Pattman for access to their clinic cohorts, and J. Coxhead (NewGene, Newcastle-upon-Tyne, UK) for assistance with Roche 454 FLX and D. Deehan for assistance with obtaining control muscle samples.

AUTHOR CONTIBUTIONS

P.F.C. designed the study and wrote the paper. B.A.I.P. designed the study, carried out the molecular analyses and wrote the paper. C.A.H. designed and carried out the mt.δ4977 assay. R.H. and D.A.P. designed the study. I.J.W. and M.S.-K. designed and performed the UDS analysis. D.C.S. designed, programmed and carried out the *in silico* modeling.

COMPETING FINANCIAL INTERESTS

The authors declare no competing financial interests.

Published online at http://www.nature.com/naturegenetics/.
Reprints and permissions information is available online at http://www.nature.com/reprints/index.html.

1. Effros, R.B. *et al.* Aging and infectious diseases: workshop on HIV infection and aging: what is known and future research directions. *Clin. Infect. Dis.* **47**, 542–553 (2008).
2. Bua, E. *et al.* Mitochondrial DNA-deletion mutations accumulate intracellularly to detrimental levels in aged human skeletal muscle fibers. *Am. J. Hum. Genet.* **79**, 469–480 (2006).
3. Trifunovic, A. *et al.* Premature ageing in mice expressing defective mitochondrial DNA polymerase. *Nature* **429**, 417–423 (2004).
4. Brierley, E.J., Johnson, M.A., James, O.F. & Turnbull, D.M. Effects of physical activity and age on mitochondrial function. *QJM* **89**, 251–258 (1996).
5. Desquilbet, L. *et al.* HIV-1 infection is associated with an earlier occurrence of a phenotype related to frailty. *J. Gerontol. A Biol. Sci. Med. Sci.* **62**, 1279–1286 (2007).
6. Oursler, K.K., Sorkin, J.D., Smith, B.A. & Katzel, L.I. Reduced aerobic capacity and physical functioning in older HIV-infected men. *AIDS Res. Hum. Retroviruses* **22**, 1113–1121 (2006).
7. Guaraldi, G. *et al.* Coronary aging in HIV-infected patients. *Clin. Infect. Dis.* **49**, 1756–1762 (2009).
8. Valcour, V. *et al.* Higher frequency of dementia in older HIV-1 individuals: the Hawaii Aging with HIV-1 Cohort. *Neurology* **63**, 822–827 (2004).
9. Lim, S.E. & Copeland, W.C. Differential incorporation and removal of antiviral deoxynucleotides by human DNA polymerase gamma. *J. Biol. Chem.* **276**, 23616–23623 (2001).

10. McComsey, G.A. *et al.* Improvements in lipoatrophy, mitochondrial DNA levels and fat apoptosis after replacing stavudine with abacavir or zidovudine. *AIDS* **19**, 15–23 (2005).
11. Côté, H.C. *et al.* Changes in mitochondrial DNA as a marker of nucleoside toxicity in HIV-infected patients. *N. Engl. J. Med.* **346**, 811–820 (2002).
12. Maagaard, A. *et al.* Mitochondrial (mt)DNA changes in tissue may not be reflected by depletion of mtDNA in peripheral blood mononuclear cells in HIV-infected patients. *Antivir. Ther.* **11**, 601–608 (2006).
13. Hayashi, J. *et al.* Introduction of disease-related mitochondrial DNA deletions into HeLa cells lacking mitochondrial DNA results in mitochondrial dysfunction. *Proc. Natl. Acad. Sci. USA* **88**, 10614–10618 (1991).
14. Corral-Debrinski, M. *et al.* Mitochondrial DNA deletions in human brain: regional variability and increase with advanced age. *Nat. Genet.* **2**, 324–329 (1992).
15. Brierley, E.J., Johnson, M.A., Lightowlers, R.N., James, O.F. & Turnbull, D.M. Role of mitochondrial DNA mutations in human aging: implications for the central nervous system and muscle. *Ann. Neurol.* **43**, 217–223 (1998).
16. Fayet, G. *et al.* Ageing muscle: clonal expansions of mitochondrial DNA point mutations and deletions cause focal impairment of mitochondrial function. *Neuromuscul. Disord.* **12**, 484–493 (2002).
17. Pereira, L. *et al.* The diversity present in 5,140 human mitochondrial genomes. *Am. J. Hum. Genet.* **84**, 628–640 (2009).
18. Lee, H.C., Pang, C.Y., Hsu, H.S. & Wei, Y.H. Differential accumulations of 4,977 bp deletion in mitochondrial DNA of various tissues in human ageing. *Biochim. Biophys. Acta* **1226**, 37–43 (1994).
19. Chinnery, P.F. & Samuels, D.C. Relaxed replication of mtDNA: a model with implications for the expression of disease. *Am. J. Hum. Genet.* **64**, 1158–1165 (1999).
20. Wanrooij, S. *et al.* Twinkle and POLG defects enhance age-dependent accumulation of mutations in the control region of mtDNA. *Nucleic Acids Res.* **32**, 3053–3064 (2004).
21. Del Bo, R. *et al.* Remarkable infidelity of polymerase gammaA associated with mutations in POLG1 exonuclease domain. *Neurology* **61**, 903–908 (2003).
22. Elson, J.L., Samuels, D.C., Turnbull, D.M. & Chinnery, P.F. Random intracellular drift explains the clonal expansion of mitochondrial DNA mutations with age. *Am. J. Hum. Genet.* **68**, 802–806 (2001).
23. Cherry, C.L. *et al.* Tissue-specific associations between mitochondrial DNA levels and current treatment status in HIV-infected individuals. *J. Acquir. Immune Defic. Syndr.* **42**, 435–440 (2006).
24. Smyth, K. *et al.* Prevalence of and risk factors for HIV-associated neuropathy in Melbourne, Australia 1993–2006. *HIV Med.* **8**, 367–373 (2007).
25. Diaz, F. *et al.* Human mitochondrial DNA with large deletions repopulates organelles faster than full-length genomes under relaxed copy number control. *Nucleic Acids Res.* **30**, 4626–4633 (2002).
26. Greaves, L.C. *et al.* Quantification of mitochondrial DNA mutation load. *Aging Cell* **8**, 566–572 (2009).
27. Kollberg, G. *et al.* Low frequency of mtDNA point mutations in patients with PEO associated with *POLG1* mutations. *Eur. J. Hum. Genet.* **13**, 463–469 (2005).
28. World Health Organization. *Antiretroviral Therapy for HIV Infection in Adults and Adolescents: A Public Health Approach.* (2006).

ONLINE METHODS

Ethics. This study was approved by the Newcastle and North Tyneside Local Research Ethics Committee. Informed consent was obtained from all subjects.

Clinical details. Clinical details are described in the **Supplementary Note**.

Histochemistry. We obtained 20 µm frozen sections from fresh-frozen lower limb skeletal muscle biopsies and placed them on polyethylene naphthalate (PEN) membrane slides (Leica) for subsequent laser microdissection. COX (cytochrome *c* oxidase) contains subunits encoded by the mitochondrial genome and stains brown (positive) in the presence of preserved respiratory chain activity. SDH (succinate dehydrogenase) provides an effective counter stain (blue), as this respiratory chain complex is entirely encoded by the nuclear genome and will be preserved in the presence of an mtDNA defect. Thus, COX-deficient fibers are predicted to contain somatic mtDNA mutations. ATPase histochemistry was performed on adjacent frozen sections in order to determine fiber type (oxidative or glycolytic).

Molecular analyses. All primers used are listed (**Supplementary Table 4**). All nucleotide positions refer to the revised Cambridge Reference Sequence (rCRS, NC_012920).

Individual skeletal muscle fibers were captured by laser microdissection (Leica) and digested in 30 µl of lysis buffer (50 mM Tris-HCl pH 8.5, 0.5% Tween-20 and 200 µg/ml proteinase K). Real-time PCR was performed as previously described[29]. Briefly, mtDNA content was determined using a target template in *MT-ND1*. When comparing COX-deficient and normal fibers, these were matched for fiber type and adjusted for fiber size. We estimated the proportion of mtDNA molecules containing large-scale deletions using a target template in *MT-ND4*. For determination of relative mtDNA content at the whole-tissue level, we performed real-time PCR as above with the inclusion of the nuclear template, *B2M*. The proportion of mtDNA molecules in muscle homogenate containing the mt.δ4977 'common deletion' were estimated by real-time PCR comparing *MT-ND1* and a product (CD) specifically amplified only in the presence of the common deletion. CD-*ND1* real-time PCR was performed in a 20 µl reaction comprising 1× Evagreen supermix (BioRad), 0.625 µM primers and 50 ng DNA. PCR protocol comprised 98 °C for 2 min, followed by 40 cycles of 98 °C for 5 s and 60 °C for 20 s. In addition to a PCR negative, DNA extracted from whole blood of a 25-year-old healthy control subject was used to define the lower limit of sensitivity for this assay, as negligible mt.δ4977 is expected to be detectable in blood by these methods[18,30].

Long-range PCR to detect mtDNA deletions in individual fibers was performed using nested PCR as previously described[31]. Deletion break points were then characterized by amplification of a ~500-bp fragment across the deletion break point. Break-point PCR reactions were performed in a 25 µl reaction containing 1× ImmoBuffer (Bioline), 2 mM $MgCl_2$, 0.2 mM dNTPs, 1 U Immolase (Bioline) and 1 µl of long-range PCR product, diluted 1:50 with PCR-grade water. PCR conditions were 95 °C for 10 min and 25 cycles of 95 °C for 15 s, 58 °C for 15 s and 72 °C for 30 s. Cycle sequencing was performed using BigDye Terminator v3.1 kit (Applied Biosystems) and visualized through a 3130× Genetic Analyzer (Applied Biosystems).

Whole-genome sequencing from individual fibers was performed based on our previous methods[32]. A nested PCR comprising a primary PCR with nine overlapping primer pairs was followed by 36 overlapping secondary PCR primer pairs. Primary PCR was performed in a 50 µl volume containing 1× PCR buffer (10 mM Tris-HCl pH 8.3, 1.5 mM $MgCl_2$, 50 mM KCl and 0.001% w/v gelatin), 1 mM $MgCl_2$, 0.2 mM dNTPs, 0.6 µM primers, 1.75 U AmpliTaq Gold (Applied Biosystems) and 1 µl lysate. PCR conditions were 94 °C for 10 min and 38 cycles of 94 °C for 45 s, 58 °C for 45 s and 72 °C for 2 min. Final extension was 8 min. Secondary PCR was performed in a 25 µl volume containing 1× PCR buffer (as above), 0.2 mM dNTPs, 0.8 µM primers, 0.65 U AmpliTaq Gold and 1 µl of primary PCR product. PCR conditions were as above except for 1 min extension and 30 cycles. Cycle sequencing was performed as above.

Ultra-deep re-sequencing by synthesis (UDS; Roche 454 GS FLX) was performed by PCR amplification of two mtDNA amplicons: one in the noncoding (control region) hypervariable segment 2 (*MT-HV2*) (amplicon position, nt 162 to nt 455, 294 bp) and one in the coding region, COX subunit 3 (*MT-CO3*) (amplicon position, nt 9,307 to nt 9,591, 285 bp). Primer specificity and lack of amplification of nuclear pseudogenes was predicted by BLAST[33] and confirmed by failure of amplification of any product from rho_0 cellular DNA. In addition we generated a nuclear DNA amplicon (*BRCA2*, NC_000013.10, 32,907,099–32,907,295). Amplicon generation was performed in a 50 µl volume containing 1× buffer for KOD Hot Start DNA Polymerase (Novagen), 1.5 mM $MgSO_4$, 0.2 mM dNTPs, 0.3 µM primers, 1 U KOD Hot Start DNA Polymerase (Novagen) and 100 ng DNA. Cycling conditions were 95 °C for 2 min followed by 30 cycles of 95 °C for 20 s, 60 °C for 10 s and 70 °C for 4 s. Emulsion PCR and sequencing were performed according to manufacturer's instructions (Roche 454). Confirmatory experiments were performed by amplicon sequencing a larger amplicon in the same regions using Roche 454 GS FLX Titanium system. Amplicon positions for Titanium assay were: *MT-HV2*, nt 109 to nt 483; *MT-CO3*, nt 9,304–9,653; *BRCA2*, 32,907,060–32,907,350. Amplicon generation PCR was as for the initial FLX assay with the exception of a 5 s extension per cycle. Repeat assays were performed for HIV−, HIV+/NRTI+ and *POLG* subjects ($n = 4$ each). Amplicons were additionally generated from cloned DNA fragments (*MT-HV2* clone, nt 16,548 to nt 771; *MT-CO3* clone, nt 9,127 to nt 9,661; *BRCA2* clone, 32,906,828–32,907,480; cloned in pGEM-T-Easy vector, Promega). An analysis pipeline of PyroBayes and Mosaik[34] was used to call and align bases from the 454 flowgram output. Subsequent analysis of variants was done in R using the custom made R library flowgram (available from the authors I.W. and M.S.K.). For comparison of samples with varying coverage depths, 5,000 sub-sampled sequences were used for all samples in all analyses. Recent studies of low-level variance in mtDNA using next-generation sequencing by synthesis technology have employed the Illumina GA platforms[35]. Experience to date suggests that this approach appears limited to a resolution of ~1–1.5% variant frequency or higher, below which true variance cannot be distinguished from noise, despite very high theoretical read depths. In order to improve on this depth of resolution, we filtered the raw FLX flowgram output for sites predicted to give poor resolution. As FLX resequencing employs pyrosequencing technology, it is prone to sequencing errors associated with mononucleotide tracts. Analysis of our outputs from cloned DNA confirmed this observation, and such sites were excluded from further analysis. Such an approach enabled resolution to variants with measured frequency ≥0.2%, whereby there was negligible variance detected in any cloned DNA amplicon or the nuclear (*BRCA2*) amplicon from genomic DNA at this level (~0.5% of base positions). Comparison with mtDNA amplicon sequence variants from patient samples thus indicated that almost all low frequency variants (>0.2%) reflect true sequence variation rather than noise. Power calculations indicate that this assay will have 80% power to detect an absolute increase in mutation burden of 2.7% at $P < 0.05$.

Modeling of NRTI effects on mtDNA replication. Modeling was performed by development of a validated simulation model of mtDNA replication and age-associated clonal expansion of mtDNA mutations based solely on experimentally derived parameters[22]. The effect of NRTIs on mtDNA replication was modeled by including a probability of failure for each replication event. In the case of a replication failure, the mtDNA molecule being copied was assumed to be destroyed. With this assumption, any failure rate of 50% or greater results in the complete loss of the mtDNA from the simulation. *De novo* mutations were modeled by including a probability of mutation formation at each replication event, with a probability of 5×10^{-5} per replication, which was kept constant across all simulated exposure groups. The *de novo* mutation rate was set at this value in order to keep the probability of forming clonal expansions below 1% before age 70 in the control case. Other relevant parameter values were the optimal mtDNA copy number (N_{opt} = 5,000), the mtDNA half life (10 days) and the maximum proliferation factor ($\alpha = 15$). Two-thousand cells were simulated to measure the probability of developing clonal expansions of mtDNA mutations. Simulated cells which fixed on the mutant (a very rare occurrence) were removed from the model. The simulation was written in FORTRAN and is available from the author (DCS).

Statistical analyses. Percentage levels of COX defect were compared between groups (≥500 fibers per subject) by Mann-Whitney test. Comparison of proportions of COX-deficient and normal fibers showing mtDNA deletions was made by χ^2 test. Comparison of mean $\log_{10}$(mtDNA) content and $\log_{10}$(CD/mtDNA) levels in skeletal muscle homogenates was made using

doi:10.1038/ng.863

a *t* test. Statistical comparisons were performed using R. The multiple regression models were run in Origin 7 (OriginLab).

29. Durham, S.E., Samuels, D.C., Cree, L.M. & Chinnery, P.F. Normal levels of wild-type mitochondrial DNA maintain cytochrome c oxidase activity for two pathogenic mitochondrial DNA mutations but not for m.3243A→G. *Am. J. Hum. Genet.* **81**, 189–195 (2007).
30. Shieh, D.B. *et al.* Mitochondrial DNA alterations in blood of the humans exposed to N,N-dimethylformamide. *Chem. Biol. Interact.* **165**, 211–219 (2007).
31. Bender, A. *et al.* High levels of mitochondrial DNA deletions in substantia nigra neurons in aging and Parkinson disease. *Nat. Genet.* **38**, 515–517 (2006).
32. Durham, S.E., Samuels, D.C. & Chinnery, P.F. Is selection required for the accumulation of somatic mitochondrial DNA mutations in post-mitotic cells? *Neuromuscul. Disord.* **16**, 381–386 (2006).
33. Altschul, S.F., Gish, W., Miller, W., Myers, E.W. & Lipman, D.J. Basic local alignment search tool. *J. Mol. Biol.* **215**, 403–410 (1990).
34. Quinlan, A.R., Stewart, D.A., Stromberg, M.P. & Marth, G.T. Pyrobayes: an improved base caller for SNP discovery in pyrosequences. *Nat. Methods* **5**, 179–181 (2008).
35. He, Y. *et al.* Heteroplasmic mitochondrial DNA mutations in normal and tumour cells. *Nature* **464**, 610–614 (2010).